THE JOURNAL OF BIOLOGICAL CHEMISTRY VOL. 287, NO. 40, pp. 33447–33459, September 28, 2012
Published in the U.S.A.

Multiplexed Activity-based Protein Profiling of the Human Pathogen *Aspergillus fumigatus* Reveals Large Functional Changes upon Exposure to Human Serum*[S]

Received for publication, June 22, 2012, and in revised form, July 27, 2012 Published, JBC Papers in Press, August 3, 2012, DOI 10.1074/jbc.M112.394106

Susan D. Wiedner[‡], Kristin E. Burnum[‡], LeeAnna M. Pederson[‡], Lindsey N. Anderson[‡], Suereta Fortuin[‡], Lacie M. Chauvigné-Hines[‡], Anil K. Shukla[‡], Charles Ansong[‡], Ellen A. Panisko[§], Richard D. Smith[‡], and Aaron T. Wright[‡1]

From the [‡]Biological Sciences Division and the [§]Chemical and Biological Processes Development Group, Pacific Northwest National Laboratory, Richland, Washington 99352

Background: *A. fumigatus* is an opportunistic pathogen responsible for pulmonary invasive aspergillosis.
Results: Multiplexed ABPP revealed significant changes in *A. fumigatus* metabolism and stress response during culture with human serum over time.
Conclusion: Changes in functional pathways indicate robust adaptation to environmental change.
Significance: *A. fumigatus* grows under stress by altering metabolism, energy production, and protein biosynthesis, which is relevant for lung colonization.

Environmental adaptability is critical for survival of the fungal human pathogen *Aspergillus fumigatus* in the immunocompromised host lung. We hypothesized that exposure of the fungal pathogen to human serum would lead to significant alterations to the organism's physiology, including metabolic activity and stress response. Shifts in functional pathway and corresponding enzyme reactivity of *A. fumigatus* upon exposure to the human host may represent much needed prognostic indicators of fungal infection. To address this, we employed a multiplexed activity-based protein profiling (ABPP) approach coupled to quantitative mass spectrometry-based proteomics to measure broad enzyme reactivity of the fungus cultured with and without human serum. ABPP showed a shift from aerobic respiration to ethanol fermentation and utilization over time in the presence of human serum, which was not observed in serum-free culture. Our approach provides direct insight into this pathogen's ability to survive, adapt, and proliferate. Additionally, our multiplexed ABPP approach captured a broad swath of enzyme reactivity and functional pathways and provides a method for rapid assessment of the *A. fumigatus* response to external stimuli.

Aspergillus fumigatus is a ubiquitous filamentous fungus found in soil and decaying matter that plays an important role in recycling carbon and nitrogen from organic debris. Provided the prevalent nature of these conidia in ambient air, it is estimated that individuals inhale hundreds of airborne conidia per day. Exposure to conidia is inconsequential if the immune system is intact, but this saprophytic fungus is an opportunistic pathogen and the leading cause of the pulmonary infection invasive aspergillosis (IA)[2] (1). Immunodeficiency associated with solid organ and allogeneic bone marrow transplantation, prolonged corticosteroid therapy, genetic immunodeficiency, HIV infection, or hematological malignancies such as leukemia increase susceptibility to this devastating disease (2). As the at risk population has increased over the past 2 decades, so too has the incidence of IA (3). Key challenges remain in understanding the biology of *A. fumigatus* responsible for infection as well as detection and treatment of IA. Techniques for reliable early stage diagnosis (4, 5), identification of IA biomarkers with prognostic value for monitoring fungal load and response to therapeutic intervention, identification of new drug targets (6), and understanding of fungal biology under infection-relevant conditions continue to be active areas of research.

Considerable effort has focused on finding and understanding the pathogenicity and virulence factors of the fungus. This opportunistic pathogen lacks true virulence factors because it evolved to break down organic matter (7). However, many characteristics contribute to its pathogenicity (1, 8), making it highly pathogenic in the immunocompromised host (7). These

* This work was supported, in whole or in part, by National Institutes of Health Grant (NIH), NCRR, Grant 5P41RR018522-10 and NIH, NIGMS, Grant 8 P41 GM103493-10. This work was also supported in part by the Laboratory Directed Research and Development Program at Pacific Northwest National Laboratory (PNNL), a multiprogram national laboratory operated by Battelle for the United States Department of Energy under Contract DE-AC05-76RL01830. This work used instrumentation and capabilities developed under support from the National Institutes of Health (Grant P41 GM103493-10) and the United States Department of Energy Office of Biological and Environmental Research (DOE/BER). Work was performed in the Environmental Molecular Sciences Laboratory, a DOE/BER national scientific user facility at PNNL.

The raw LC-MS/MS data and SEQUEST search results for all biological replicates and culture conditions have been deposited in the Biological MS Data and Software Distribution Center data repository under publication number 1057. The data can be accessed at http://omics.pnl.gov/view/publication_1057.html.

[S] This article contains supplemental Tables S1–S10 and Figs. S1–S5.

[1] Recipient of the PNNL Linus Pauling Distinguished Postdoctoral Fellowship. To whom correspondence should be addressed: Biological Sciences Division, Pacific Northwest National Laboratory, 902 Battelle Blvd., Richland, WA 99352. E-mail: aaron.wright@pnnl.gov.

[2] The abbreviations used are: IA, invasive aspergillosis; ABPP, activity-based protein profiling; ABP, activity-based probe; AMT, accurate mass and time; HS, human serum; fc, fold change; AMM, *Aspergillus* minimal medium; ROS, reactive oxygen species; gcl, global cell lysate.

include its environmental and metabolic adaptability: *A. fumigatus* grows rapidly at high temperatures and within hypoxic conditions (9, 10); it can obtain carbon and nitrogen from diverse sources (11, 12); and it is highly adaptive in its ability to uptake nutrients from its environment (13). We utilized a chemical biology approach to characterize the fungal functional adaptation to changes in nutrient availability in conditions relevant to IA infection.

Global proteome analysis of *A. fumigatus* has elucidated protein regulation and pathway responses to environmental stimuli (14). However, global (*i.e.* untargeted) proteomics provides incomplete proteome coverage and generally fails to provide quantifiable measurement of the functional activity of observed proteins because proteins are dynamic and highly regulated and often exist in inactive forms until proteolytically processed or post-translationally modified. Activity-based protein profiling (ABPP) has emerged to overcome the inherent difficulty of differentiating presence *versus* activity and to facilitate the measurement of low abundance reactive proteins. ABPP employs specific chemical probes to observe the active protein complements of biological systems (15, 16). Synthetic activity-based probes (ABPs) inhibit enzymes by forming an irreversible covalent bond to the enzyme active site. Enriching and identifying ABP-tagged proteins allows proteomic annotation of function, reduces the complexity of the proteome under analysis, and measures low abundance functional proteins. Coupled with high throughput, high resolution LC-MS/MS analysis utilizing a quantitative accurate mass and time (AMT) tag approach (17), environmental adaptation and metabolic response can be quantified using ABPP.

During the course of IA, *A. fumigatus* hyphae breach host tissue and interact with serum. *A. fumigatus* is one of the few pathogenic organisms that readily grows in the presence of serum (18) due to its ability to extract iron from human transferrin in this iron-limited environment (19). Furthermore, *A. fumigatus* can use serum proteins for biomass generation (20, 21), but the full effect of serum on the cellular processes of *A. fumigatus* and its relevance to disease is not fully understood. We hypothesize that *A. fumigatus* can adapt to this nutrient source for metabolic purposes and that fungal enzyme activity within human serum (HS) will be relevant to its metabolism, nutrient sensing, and scavenging response within the immunocompromised host environment. This information can provide valuable insight into how *A. fumigatus* survives in a host environment on a fundamental biological process level. Herein, we describe a novel ABP and label-free quantitative multiplexed ABPP methodology for delineating the protein activity of *A. fumigatus* during growth in minimal medium in response to HS as a function of growth duration.

EXPERIMENTAL PROCEDURES

Synthesis of Activity-based Probes 1 and 2—Detailed experimental procedures for the synthesis of **1** and **2** are available in the supplemental material.

Strains, Media, and Culture Conditions—*A. fumigatus* ATCC® MYA-4609™ (AF 293) obtained from ATCC were stored at −80 °C in individual glycerol. Potato dextrose agar plates were inoculated with conidia from glycerol stocks and harvested by flooding the plate with 0.8% Tween 80 after 4 days. The conidia suspension was filtered through Miracloth (Calbiochem), and the conidia were counted by hemocytometer. For liquid culture, complete *Aspergillus* minimal medium (AMM; 1% glucose, 2 ml/liter Hunter's trace elements) (22) with or without 10% HS was inoculated to a final concentration of 1×10^6 conidia/ml. Biomass was grown at 37 °C and agitated at 150 rpm on an orbital shaker for 24 or 48 h.

Human Serum—HS (Sigma) was stored at −20 °C and used without further processing.

Growth Curve—AMM and AMM containing 10% HS were inoculated to 1×10^6 conidia/ml with *A. fumigatus* and cultured as described above. Fungal biomass was harvested in triplicate at each time point by filtering the liquid culture through Miracloth, washing the collected biomass with water, and cryodessication. The mass of the dried fungus was used to generate a growth curve (Fig. 1).

Cell Lysis—Biomass was harvested at 24 and 48 h and passed through Miracloth to remove spent medium, and the retained biomass was washed with 15 ml of PBS. Excess medium was squeezed out of the biomass. The biomass was manually cut and then lysed with a Bullet Blender (NextAdvance): 0.55-mm zirconium silicate beads (0.5–1.0 ml) and PBS (1–2 volumes) (1×, pH 7.4: 11.9 mM phosphates, 137 mM NaCl, 2.7 mM KCl) per 5-ml tube. Lysed samples were centrifuged at 3,500 × *g* for 5 min, pellets were washed with PBS (1 ml) and spun at 3,500 × *g* for 5 min, and the combined supernatants were spun twice more. Sonication of the final combined supernatant provided global cell lysate (gcl). The gcl was flash frozen in liquid nitrogen and stored at −80 °C until further use. All material was generated in quadruplicate.

Enzyme Assays—Using a BCA assay, the protein concentration of gcl from AMM + HS 24- and 48-h growth was then normalized to 1 mg/ml protein (supplemental Fig. S1*A*). Alcohol dehydrogenase activity for the gcl was measured as described previously (23). The assay was performed in triplicate, and the slope was calculated using data points from 3–6 min (supplemental Fig. S1*C*). Citrate synthase activity was measured with a commercial kit (Sigma-Aldrich); assays were run in triplicate (supplemental Fig. S1*B*).

In Vitro Probe Labeling for Mass Spectrometry Measurement—*A. fumigatus* mycelia lysate proteomes (1 mg/ml in PBS) were treated with vinyl sulfonate **1** (20 μM) and fluorophosphonate **2** (200 μM) in a 1.5-ml vial and incubated for 1 h at 37 °C. Following probe incubation, proteomes were treated with click chemistry reagents and enriched by the method of Cravatt with the following changes. Peptides were obtained by treating the resin with trypsin (2 μl; trypsin was reconstituted in 40 μl of NH_4HCO_3 (25 mM, pH 8)) and NH_4HCO_3 (25 mM, pH 8; 200 μl) and subsequent incubation at 37 °C, 1,200 rpm, for 15 h. Following digestion, peptide supernatant was obtained (6,000 × *g*), and the pellet was washed with NH_4HCO_3 (25 mM, pH 8; 150 μl). The combined peptide supernatant was dried by speed vacuum, reconstituted in NH_4HCO_3 (25 mM, pH 8; 40 μl), and heated for 10 min at 37 °C. The samples were centrifuged at 100,000 × *g* for 20 min at 4 °C, and 25 μl was collected for MS analysis.

LC-MS Measurement of ABP-labeled Proteins—Digested peptide mixtures were measured on a Thermo Fisher Scientific LTQ Orbitrap Velos MS (San Jose, CA) as described previously (24). The Velos MS data were collected from 400 to 2,000 m/z at a resolution of 100,000 (automatic gain control target: 1×10^6) followed by data-dependent ion trap MS/MS spectra (AGC target: 1×10^4) of the 10 most abundant ions using a collision energy setting of 35–40% and a dynamic exclusion time of 30 or 180 s.

Significant changes were determined at the unique peptide level between growth conditions or culture durations. The resulting MS data were analyzed using the AMT tag pipeline to determine relative protein abundance (17). SEQUEST software (25) was used to search tandem mass spectra against the UniProt *A. fumigatus* database (April 1, 2011). Peptide identifications filtered with an MS-generating function spectral probability score of $\leq 1 \times 10^{-9}$ (26) were assembled into an *A. fumigatus*-specific AMT tag database. For identification, VIPER software (27) was used to correlate each AMT tag entry with a unique LC-MS feature relying on high mass measurement accuracy ($MMA_{average} \pm 0.683$ ppm) and normalized elution time accuracy ($NET_{average} \pm 0.363\%$) (supplemental Tables S1–S4). Single peptides matching multiple proteins (typically protein isoforms) were removed. Proteins increasing in the presence of HS were manually verified to originate from fungus by looking at MS/MS scans (supplemental Table S5).

For statistical analysis of peptide abundance, DAnTE software (28) was used to perform ANOVA significance tests on culture comparisons; a significant difference was determined as a p value and q value of <0.05. The q value of a test measures the proportion of false positives incurred (*i.e.* the false discovery rate) for the analysis. Significant peptides found in at least three data sets were rolled up into protein values using Rrollup (28). An absolute -fold change (|fc|) of ≥ 15, ≥ 2 peptides/protein, and $\geq 10\%$ protein coverage were used to ensure high confidence of significantly changing proteins. Unique proteins were obtained by rolling up all unique peptides to protein and using a relative abundance cut-off of ≥ 18, ≥ 2 peptides/protein, and 10% protein coverage. Proteins were mapped to function using tools from the Aspergillus Genome Database (29), the Fungifun tools at Omnifung (30), and the KEGG pathway user mapping tool (31).

RESULTS

Growth in the Presence and Absence of Human Serum—Collection of fungal biomass at multiple time points within each culture showed strikingly different growth patterns for *A. fumigatus* in the presence and absence of 10% HS (Fig. 1). Culture with HS caused a large increase in biomass generation at 24 and 48 h. In the presence of HS, the fungus reaches log phase growth at 16 h, whereas in minimal medium, log phase growth is delayed until 24 h. At 48 h after liquid culture inoculation, *A. fumigatus* has reached stationary phase in the presence of human serum but is still in log phase growth in minimal medium. In AMM, *A. fumigatus* reaches stationary phase at 64 h. The decrease in biomass at subsequent time points corresponds to autolysis and death of the mycelia from nutrient deprivation or mechanical shearing forces that break down hyphae as the culture ages (32).

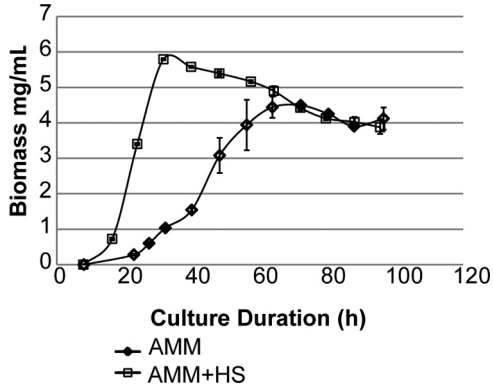

FIGURE 1. **Growth curve generated for AMM and AMM + 10% HS culture.** Biomass was harvested, flash-frozen, dried, and then weighed. Data points were collected in triplicate, and *error bars* represent S.E. of each data point.

ABP Development and One-dimensional Gel Analysis—In developing a library of known and novel ABPs that incorporate the click chemistry-compatible alkyne moiety for attachment of azide-derivatized reporter groups, we synthesized vinyl sulfonate ester probe **1** (Fig. 2*A*). The clickable alkyne probe **1** was synthesized in four steps from commercially available 4-hydroxybenzyl alcohol (33). Optimized labeling conditions of *A. fumigatus* samples were performed at a final probe concentration of 20 μM at 37 °C for 1 h (supplemental Fig. S2); these labeling conditions were used for all further analysis with **1**. Vinyl sulfonate esters are known to irreversibly inhibit cysteine proteases; however, broad labeling of distinct enzyme classes with **1** at 37 °C occurred (supplemental Fig. S2). Furthermore, treatment of purified enzymes and *A. fumigatus* gcl with 40× cysteine-reactive *N*-ethylmaleimide followed by probe labeling did not completely eradicate labeling with probe **1**, suggesting covalent binding to nucleophilic amino acids other than cysteine in the probe labeling event (Fig. 3*A* and supplemental Fig. S3), which is akin to prior electrophilic ABP reports (34–36). The generality of **1** allows interrogation of a large system-wide subset of functionally active proteins in *A. fumigatus.*

To include coverage of serine hydrolases, a serine hydrolase-specific probe (**2**) was included in the analysis of *A. fumigatus* (Fig. 3*A* and supplemental Fig. S5). Probe **2** contains a fluorophosphonate reactive group selective for serine hydrolases (37) and an alkyne for appending a reporter group (Fig. 2*B*). A probe concentration of 200 μM was optimal for labeling (supplemental Fig. S4). Probes **1** and **2** were used simultaneously to analyze the proteome of *A. fumigatus* grown with and without HS for 24 and 48 h. Because both probes contain the clickable alkyne tag, it is possible to conjugate both probes with one type of reporter group (*i.e.* biotin azide or rhodamine azide) using click chemistry. Multiplexing the ABPs permits broader coverage in a single MS measurement.

Protein labeling by ABPs was independent of protein abundance. Equivalent volumes of gcl obtained from *A. fumigatus* in the presence and absence of HS over time were labeled with **1** and **2** (Fig. 3*B*). The extent of labeling of the AMM grown samples at both time points was much greater than labeling of the AMM + HS samples (Fig. 3*B*). In culture with HS, probe label-

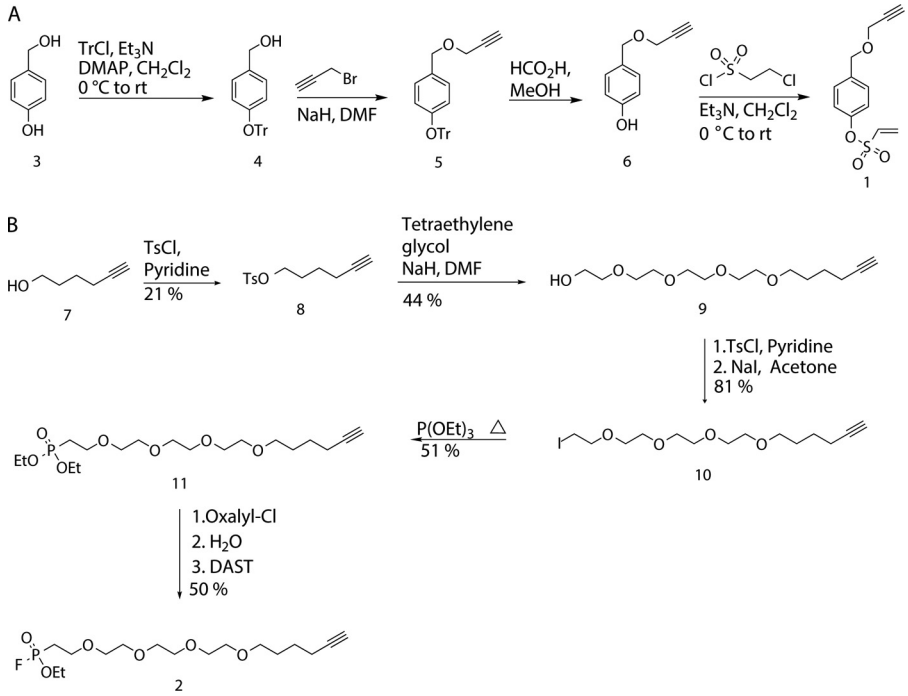

FIGURE 2. **Synthesis of vinyl sulfonate ester 1 and fluorophosphonate 2 ABPs used for multiplexed ABPP.** *A*, vinyl sulfonate ester ABP **1** was synthesized in four steps from 4-hydroxybenzyl alcohol. *B*, fluorophosphonate ABP **2** was synthesized in eight steps from 5-hexyn-1-ol. *rt*, room temperature. *DMF*, dimethylformamide; *DMAP*, 4-dimethylaminopyridine; *DAST*, diethylaminosulfur trifluoride.

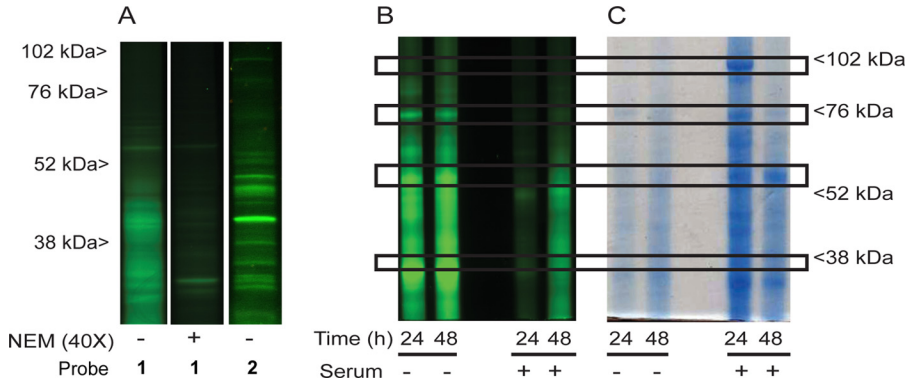

FIGURE 3. **Labeling of gcl of *A. fumigatus* with 1 and 2 in the presence and absence of HS at 24 and 48 h.** *A*, labeling of AMM + HS 48 h gcl with **1** in the presence and absence of 40× *N*-ethylmaleimide (*NEM*) showed incomplete labeling inhibition, suggesting nucleophilic attack of **1** by non-cysteine amino acids. A distinct labeling pattern AMM + HS 48 h gcl is observed when **2** is used. *B*, one-dimensional SDS-PAGE fluorescent image of *A. fumigatus* gcl labeled with **1** and **2** showed the highest probe reactivity in AMM at 24 h (*lane 1*) and 48 h (*lane 2*). Lower enzyme reactivity was observed in AMM + HS at both time points (*lanes 3* and *4*). *C*, Coomassie-stained image of *A. fumigatus* gcl labeled with probes 1 and 2 showed that labeling was not dependent on protein abundance. The highest protein content corresponded to the lowest fluorescent labeling. *Boxes* at 102, 76, 60, and 38 kDa show the discrepancy between protein abundance and protein labeling.

ing was greater at 48 h than at 24 h. Strikingly, Coomassie protein staining of the gel showed higher protein content in AMM + HS samples than in the AMM samples, but probe labeling was lower (Fig. 3*C*). Three highly abundant proteins by protein staining in AMM + HS 24 h at 60, 80, and 102 kDa were not ABP-labeled. Later time points (4 days) showed a significant overall reduction in enzyme reactivity (supplemental Fig. S4).

Our data clearly indicate that **1** and **2** probe different enzyme reactivity, and labeling is independent of protein abundance. Although probe and protein interaction at a non-catalytic residue within the active site or a ligand binding site with an adjacent nucleophile cannot be ruled out at this time (38, 39), the differences in enzyme reactivity (fluorescent intensity) suggest that there is a different functional state of the tagged enzymes between conditions. If probe labeling was not determined by enzyme functional state, we would expect to see labeling of all proteins within a sample. Therefore, we relate the observed changes in enzyme reactivity with differences in functional activity between the samples.

ABPP by LC-MS and LC-MS/MS—Global cell lysates of *A. fumigatus* grown in the presence and absence of HS and labeled with **1** and **2** were analyzed by LC-MS/MS, and LC-MS features were identified using quantitative peak matching to an AMT tag database (17). Using the above described criteria, the relative abundance of confident protein identifications were compared over time and growth conditions. When comparing protein abundance between conditions, an absolute fc cut-off of

TABLE 1

Protein trends between conditions

Proteins with high, low, and no fold change between conditions. All proteins counted have >10% peptide coverage and >1 peptide per protein. A *p*-value >0.05 was used to determine proteins with no significant fold change. The symbol | denotes absolute value of the fold change value. A negative value denotes greater reactivity in condition B, and a positive value denotes greater reactivity in condition A. For unique proteins, a Log_2 abundance of >18 was required. For a complete list of proteins and peptides observed in this comparison, see Table S1, S2, S3, S4.

Condition A	Condition B	Non-changing (A/B)	|fc| > 2 (A/B)	|fc| < 15 (A/B)	fc >15 (A/B)	Unique to A	Unique to B
AMM + HS 24 h	AMM 24 h	196	242	81	1	0	6
AMM + HS 48 h	AMM 48 h	166	345	27	0	3	21
AMM 48 h	AMM 24h	204	342	0	23	6	0
AMM + HS 48 h	AMM + HS 24 h	44	320	0	88	10	0

15 was chosen for manual pathway analysis to ensure high confidence of measured changes and relevance of the reactive proteins to the culture conditions. Multiple enzyme families, including oxidoreductases, transferases, lyases, hydrolases, isomerases, and ligases, were identified in global cell lysates using ABPP.

Comparison of AMM 24 h to AMM + HS 24 h—We compared reactive enzyme abundance in the presence or absence of HS at 24 h (Table 1 and supplemental Table S1). At 24 h, 239 proteins had an fc less than −2 (negative value denotes higher reactivity in AMM 24 h). Eighty-two proteins had a large enzyme reactivity difference ($|fc| > 15$); only one protein (acetyl-CoA carboxylase; Table 2) had higher enzyme reactivity in the presence of HS, six proteins were observed only in the absence of HS, and 81 proteins had high levels of enzyme reactivity in AMM only (Table 1 and supplemental Table S6). Mapping proteins with absolute value $|fc| \geq 15$ onto Functional Catalogues (FunCat) showed enrichment of metabolism, protein synthesis, and energy functional categories (30) (Fig. 4 and supplemental Table S6). KEGG pathway mapping showed enrichment of genetic information processing, metabolism, and cellular processes (supplemental Table S6).

Comparison of AMM 48 h with AMM + HS 48 h—At 48 h, 340 proteins were significantly different between conditions ($|fc| > 2$), and 51 of these proteins had high enzyme reactivity ($|fc| > 15$) (supplemental Table S7), 21 were unique to and 27 had higher reactivity in AMM; three were unique to AMM + HS. The enzymes unique to growth in HS were aldehyde reductase *akr1* (AFUA_6G10260), glutathione oxidoreductase *glr1* (AFUA_1G15960), and a conserved hypothetical protein (AFUA_2G10170) (Table 2). FunCat mapping of all highly reactive proteins in the 48-h growth comparison corresponded to enrichment of protein synthesis, proteins with binding requirements, and cellular transport functions (Fig. 4 and Table S7). Two proteins involved in cell cycle regulation, histone H3 (AUFA_1G13790) and sulfur metabolism regulator *SkpA* (AFUA_5G06060), had higher ABP probe reactivity in AMM (29).

Comparison of AMM 24 h with AMM 48 h—A time comparison of AMM growth (24 h *versus* 48 h) showed 204 proteins with no significant change; at 48 h of growth, 342 proteins had a 2-fold increase in enzyme reactivity (Table 1 and supplemental Table S8), 23 proteins had a >15-fold increase, and six proteins were unique. Metabolism was highly enriched, whereas secondary metabolism was the highest enriched subcategory; in addition, detoxification subcategories were also enriched (Fig. 4 and supplemental Table S8). Five proteins with a >15-fold change are annotated with secondary metabolism function (Table 2): catalase *fgaCat* (AFUA_2G18030), active in fumigaclavine C biosynthesis (40), two melanin conidial pigment biosynthetic proteins *Arp2* (AFUA_2G17560) and *Ayg1* (AFUA_2G17550) (41), hybrid PKS-NRPS enzyme *nrps14* (AFUA_8G00540) of the pseurotin A biosynthesis gene cluster (42), and glutathione *S*-transferase (AFUA_4G14380) located on chromosome 4 near other secondary metabolite biosynthesis gene clusters (Table 2) (43). Transcription of *fgaCat*, *nrps14*, and the glutathione *S*-transferase changed in the presence of voriconazole (44) and/or hypoxic conditions (45). In addition, melanin is essential for cell wall integrity and protection against neutrophil-mediated phagocytosis (46). Finally, the proteins *mpkA* (AFUA_4G13720) and squalene monoxygenase *erg1* (AFUA_5G07780), both associated with cell wall signaling (47) and membrane synthesis (48), respectively, have altered transcription levels in response to chemical stress (29). ABP-tagged proteins associated with primary metabolic functions were still increasing, albeit with a |fc| of ~5. In AMM, proteins associated with secondary metabolism and stress response dramatically increased over time (supplemental Table S8).

Comparison of AMM + HS 24 h with AMM + HS 48 h—In the presence of HS, 44 proteins showed no difference between 24 and 48 h, a total of 320 proteins had a 2-fold increase in reactivity, and 10 proteins were unique to and 88 were highly active at 48 h of growth ($fc \geq 15$) (Table 1 and supplemental Table S4). The most highly enriched functional categories at 48 h were metabolism (31%) and energy (14%) (Fig. 4 and supplemental Table S9) (30). Furthermore, amino acid and carbohydrate metabolism were the most significant KEGG pathway annotations (supplemental Table S9) (31). The functional categories enriched at 48 h in HS culture (24 h *versus* 48 h) were also highly enriched at 24 h in minimal medium (AMM 24 h *versus* AMM + HS 24 h), including transcription, metabolism, energy, protein fate, biogenesis of cellular components, cell cycle, and DNA processing and transport (supplemental Table S9) (Fig. 4).

Validation of ABPP by Global Proteomics—To validate ABPP of filamentous fungus, we analyzed gcl obtained from AMM and AMM + HS growth at 24 h without ABP labeling. A total of 647 proteins were confidently identified between the two sample types (Fig. 5 and supplemental Table S10). Of these, 409 and 451 proteins were also detected in the functionally enriched AMM and AMM + HS samples, respectively, but 152 and 82 confident proteins (AMM and AMM + HS, respectively) were not observed in the global analysis. For example, the MAPK *MpkA* was confidently identified in the enriched AMM and

TABLE 2

Subset of proteins with metabolic, stress response, secondary metabolism, and cell cycle regulation annotation across all comparisons

Subset of proteins with metabolic, stress response, secondary metabolism, and cell cycle regulation annotation across all comparisons. NA, protein was not detected with confidence in one of the growth conditions and therefore a fold change could not be calculate; NS, no significant change between conditions (p-value > 0.05). For a complete list of proteins and peptides fold changes, see Tables S1–S4.

Protein description	Locus tag	Enzyme (EC)	-Fold change 24 h (HS/no HS)	-Fold change 48 h (HS/no HS)	-Fold change No HS (48 h/24 h)	-Fold change HS (48 h/24 h)
Histone H3	AFUA_1G13790		−9.3	−17.6	4.3	2.6
Acetyl-CoA carboxylase	AFUA_2G08670		15.4	NS[a]	13.8	3.1
Sulfur metabolism regulator SkpA	AFUA_5G06060		−20.9	−16.4	NS	3.3
Squalene monooxygenase Erg1	AFUA_5G07780		NS	NS.	19.0	4.6
Citrate synthase (Cit1)	AFUA_5G04230		−13.8	−3.6	NS	11.4
MAPK MpkA	AFUA_4G13720	2.7.11.1	NS	NS	18.8	15.5
HAD superfamily hydrolase	AFUA_5G08270		−14.78	−8.6	26.3	57.6
Alcohol dehydrogenase	AFUA_7G01010	1.1.1.1	−145.6	−8	4.5	73.7
Aldehyde reductase (AKR1)	AFUA_6G10260	1.1.1.2	NA[b]	AMM + HS only	NA	48 only
Glutathione oxidoreductase Glr1	AFUA_1G15960	1.8.1.7	NA	AMM + HS only	NA	48 only
Conserved hypothetical protein	AFUA_2G10170		NA	AMM + HS only	NA	48 only
Conserved hypothetical protein	AFUA_8G00430		AMM only	−2.9	19	NS
Flavin-binding monooxygenase-like protein	AFUA_4G09220		NS	−2.9	16.5	NS
O-Methyltransferase GliM-like	AFUA_3G12910	2.-.-.-	NS	NS	19.6	NS
Conidial pigment biosynthesis protein Ayg1	AFUA_2G17550		NS	NS	22.5	NS
Oxidoreductase, 2OG-Fe(II) oxygenase family	AFUA_3G00800		NS	NS	24.5	NS
Conidial pigment biosynthesis 1,3,6,8-tetrahydroxynaphthalene reductase Arp2	AFUA_2G17560		NS	NS	25.2	NS
Glutathione *S*-transferase	AFUA_4G14380		NS	NS	47.5	NS
Cytochrome P450 oxidoreductase OrdA-like	AFUA_8G00510		NS	NS	50.5	NS
Glutathione *S*-transferase Ure2-like	AFUA_4G14530		NS	NS	78.9	NS
Fructosyl amino acid oxidase	AFUA_6G03440		NS	NS	48 honly	NS
Catalase Cat	AFUA_2G18030	1.11.1.6	NA	AMM only	48 honly	NA
Cytochrome P450	AFUA_5G02610	1.14.-.-	NA	AMM only	48 honly	NA
Hybrid PKS-NRPS enzyme	AFUA_8G00540		NS	NS	28.3	NA

[a] NS, not significant; p-value > 0.05.
[b] NA, not applicable.

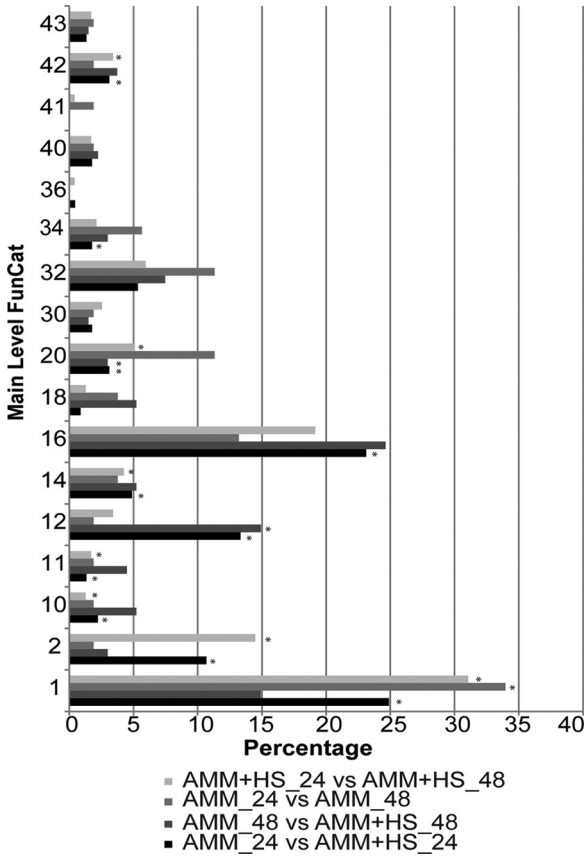

FIGURE 4. **FunCat annotation of |fc| ≥ 15 enzymes in all comparisons.** FunCat main categories are on the *y* axis, and the percentage that each category contributes to total mapping is on the *x* axis. FunCat categories are as follows: 1, metabolism; 2, energy; 10, cell cycle and DNA processing; 11, transcription; 12, protein synthesis; 14, protein fate; 16, protein with binding function or cofactor requirement; 18, regulation of metabolism and protein function; 30, cellular communication/signal transduction mechanism; 32, cell rescue, defense, and virulence; 34, interaction with the environment; 36, systemic interaction with the environment; 40, cell fate; 41, development; 42, biogenesis of cellular components; 43, cell type differentiation. *, categories found to have a *p* value of <0.05. For complete annotation mapping, see supplemental Tables S6–S9.

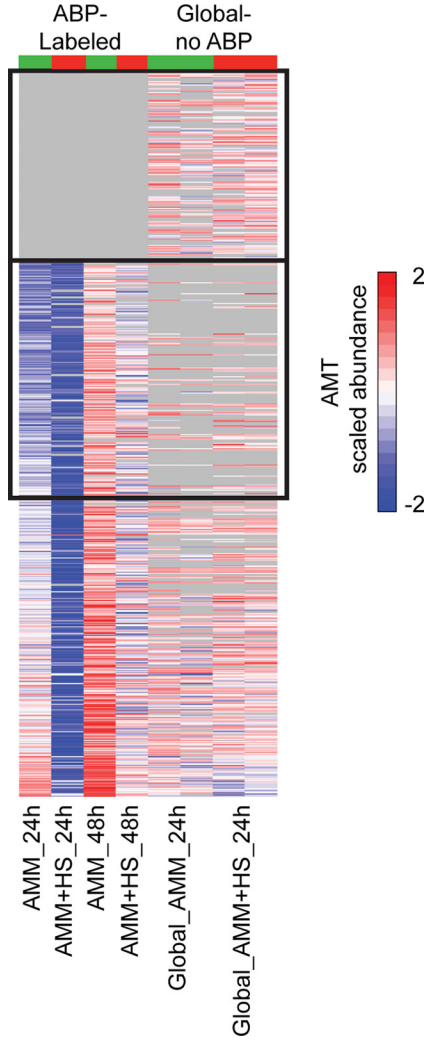

FIGURE 5. **Global ABPP and LC-MS analysis of *A. fumigatus* from AMM 24 h and AMM + HS 24 h culture.** Shown is a comparison of all functionally enriched proteins with the global untargeted proteome analysis of gcl at 24 h. Abundance values are scaled such that a range of −2 to 2 (*dark blue* to *dark red*) represents a relative intensity difference of 17 ($\log_2$). Each enriched column represents the average of at least three biological replicates. *Boxes* denote ~200 proteins observed in global analysis that were not observed in the ABPP analysis and ~100 proteins observed in ABPP samples that were not observed in global analysis. Differences in reactive protein abundances between ABPP samples correlate to gel-based analysis. See supplemental Table S10 for expanded details.

AMM + HS samples (~15% coverage) but not in the global analysis samples (<10% coverage). The disparity between confident identifications in the global and functionally enriched samples confirms that we are observing a subset of proteins based on enzyme reactivity and not simply protein abundance.

To further validate the mass spectrometry data, alcohol dehydrogenase and citrate synthase enzyme assays were performed. By MS analysis, a >15-fold change was observed in the alcohol dehydrogenase (AFUA_7G01010, EC 1.1.1.1) reactivity over time in HS culture (supplemental Table S4*A*). The alcohol dehydrogenase assay showed a 2-fc in alcohol dehydrogenase activity between 24 and 48 h in AMM + 10% HS culture (Table 3). The assay confirmed higher enzyme reactivity in the 48-h culture, but the fc observed by spectrophotometric techniques was much lower than in MS-based analysis. The fc difference is attributed to the higher resolution of MS-based measurements. Citrate synthase (AFUA_5G04230, EC 2.3.3.8, fc = 11.4) activity also increased over time by 2-fold in human serum culture according to the colorimetric enzyme assay (Table 3), which confirms the MS data showing that citrate synthase reactivity is higher in AMM + HS at 48 h (supplemental Table S4*A*). These enzyme assays independently confirm the ABPP and quantitative AMT tag analysis approach.

TABLE 3

Enzyme assay results

Enzyme assay results for citrate synthase and alcohol dehydrogenase in the AMM+HS_24 h to AMM+HS_48 h comparison. Units, μmole/ml/min. Time point absorbance was obtained in triplicate, and Student's *t*-test was applied for each data point. Citrate synthase, *p*-value < 0.05; alcohol dehydrogenase, *p* value < 0.1. Units, μmole/ml/min.

Enzyme	AMM + HS 24 h	AMM + HS 48 h	-Fold change (48 h/24 h)
	units	*units*	
Citrate synthase	0.04	0.06	1.5
Alcohol dehydrogenase	0.008	0.019	2.4

In an effort to visualize changes occurring over time in the presence and absence of HS, confidently identified proteins

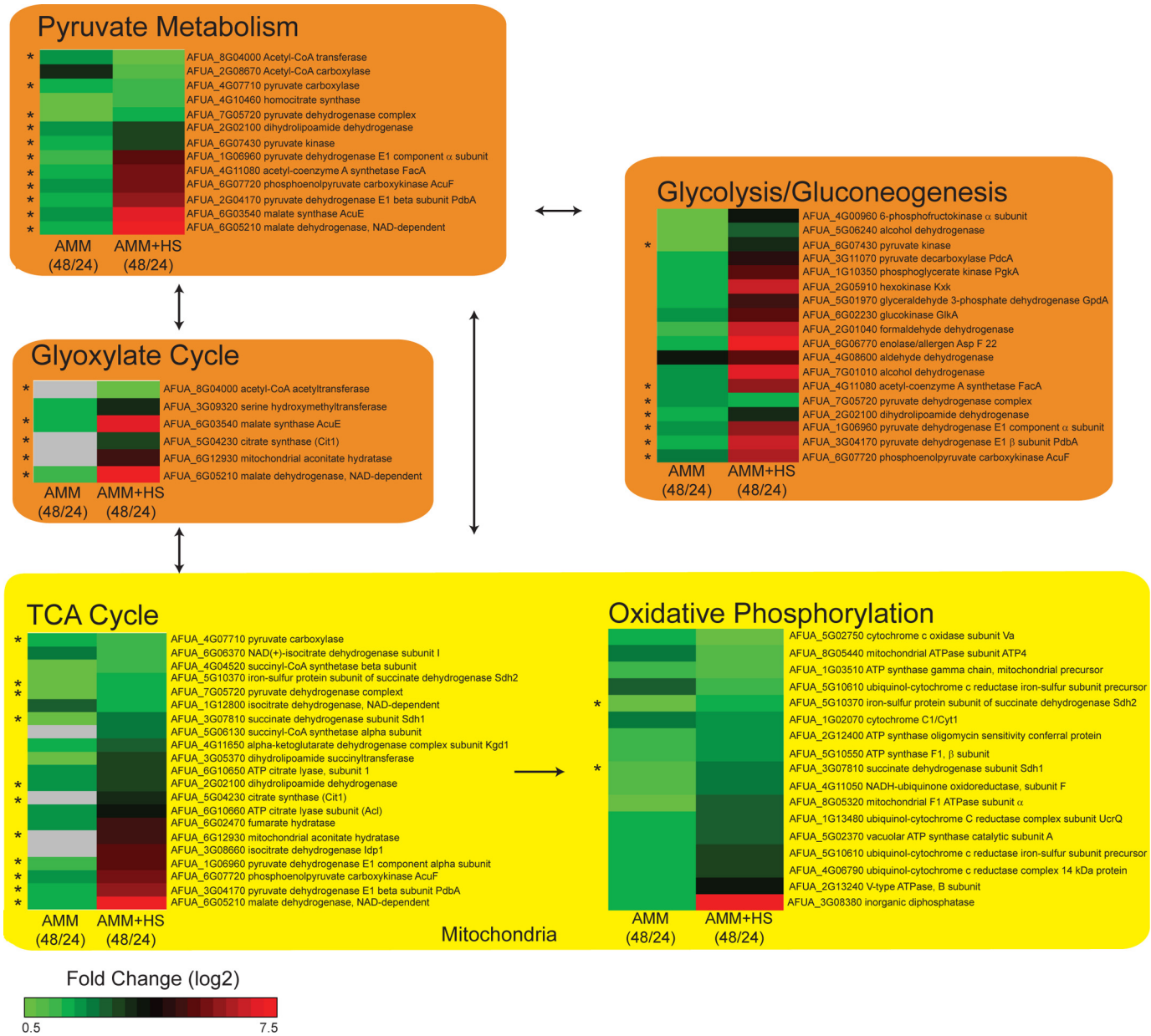

FIGURE 6. **KEGG pathway analysis.** All proteins with |fc| > 2 were mapped onto KEGG glycolysis/gluconeogenesis, TCA cycle, pyruvate metabolism, glyoxylate cycle, and oxidative phosphorylation pathways. The *yellow color* indicates processes occurring in the mitochondria, and the *orange* represents processes occurring in the cytosol. *Arrows* between pathways indicate that pathway products are used in other pathways. The *heat maps* within each pathway represent -fold change of 0.5–7.5 (log_2 scale) calculated for enzyme reactivity over time for each condition (*i.e.* AMM + HS 24 h *versus* AMM + HS 48 h and AMM 24 h *versus* AMM 48 h). *Gray boxes* represent proteins that did not make a 10% protein coverage cut-off. *, protein maps to more than one KEGG pathway.

were mapped onto KEGG pathways. We found 100, 56, 44, 55, and 14% coverage of the TCA, glycolysis/gluconeogenesis, pyruvate metabolism, glyoxylate, and oxidative phosphorylation pathways, respectively (Fig. 6) when all proteins with an |fc| of >2 were used. ABPP revealed that primary metabolism and energy production significantly increase as the fungus ages in HS culture, whereas in minimal medium, the increase of enzyme reactivity within these pathways is much lower. Reactivity is protein dependent, not pathway dependent, as can be seen by negative and positive fc within a particular pathway. This reveals that some steps within a pathway may be more active than others and provides insight into fundamental processes. For example, the alcohol dehydrogenase (AFUA_7G01010) and pyruvate decarboxylase PdcA (AFUA_3G11070), both involved in fermentation within the glycolysis pathway, have higher fc between time points than dihydrolipoamide dehydrogenase (AFUA_2G02100) involved in acetyl-CoA production.

DISCUSSION

ABPP provides a means for the functional enrichment of a biological system by chemical probe interrogation. Herein, the two new employed ABPs included a general vinyl sulfonate electrophile and a serine hydrolase-selective fluorophosphonate as reactive groups to target functional enzymes and click chemistry-compatible alkynes for downstream fluorescent or

LC-MS/MS-based reporting of ABP-labeled enzymes. Probes were used simultaneously in a multiplexed fashion to facilitate efficient use of material and mass spectrometry instrumentation. Multiplexed ABPP of *A. fumigatus* using **1** and **2** resulted in the isolation of multiple protein families from a complex proteome. Vinyl sulfonate esters react with cysteine residues by Michael addition of the sulfur to the electrophilic vinyl sulfonate (49). Furthermore, an azide derivative of **1** inhibited cysteine-dependent protein phosphatases (33). Usage of the general cysteine-reactive vinyl sulfonate ester and serine hydrolase-specific ABPs allowed enrichment of reactive proteins independent of protein abundance.

ABPP of *A. fumigatus* over two cross-culture (AMM *versus* AMM + HS) and temporal comparisons (24 h *versus* 48 h) showed two key trends; 1) higher enzyme reactivity was always observed in minimal medium, and 2) enzyme reactivity increased over time regardless of growth condition. Within these trends, we observed fluctuations in primary metabolic activity, energy production, and stress response pathways. We hypothesized that growth of the fungus in HS would promote nutrient scavenging and limit *de novo* biosynthesis due to available proteins and lipids in serum because *A. fumigatus* can adapt to changing nutrient availability (7). *A. fumigatus* can use amino acids as both carbon and nitrogen sources, and it can degrade extracellular material by proteinase excretion and uptake of degradation products (13). HS contains 60–80 mg of protein/ml and salts, lipids, amino acids, and sugars, all of which can be utilized by *A. fumigatus* (50). Indeed, the growth curve generated during this study shows that in liquid culture, the presence of HS induces early logarithmic growth and increases the production of fungal biomass (Fig. 1).

The addition of HS to the culture medium induced a large shift in functional enrichment of *A. fumigatus* proteins. At both early and late time points, enzyme reactivity was lower in the presence of HS when compared with minimal medium. Two factors may influence the higher enzyme reactivity pattern for AMM culture. First, in minimal medium, the fungus must synthesize all necessary components for growth instead of acquiring them from sera as exemplified by the delay in log phase growth for AMM culture (Fig. 1). Second, Cagas *et al.* (51) observed high expression of proteins associated with translation and aerobic respiration during early culture when compared with conidia. According to the growth curve, AMM culture is in an earlier phase than HS culture, which may result in higher translation and metabolic activity as the fungus approaches log phase (32).

In HS culture, low reactivity of enzymes associated with aerobic metabolism and protein biosynthesis is consistent with low mRNA levels found in *A. fumigatus* germlings from murine lung infection (52). Whereas enzyme reactivity associated with metabolic pathways was low at 24 h, enzyme reactivity associated with protein biosynthesis and cell cycle regulation were low at 48 h (Table 2), which is consistent with logarithmic *versus* stationary growth. During log phase growth, most of the organism biomass is dedicated to hyphae elongation, cellular component generation, and transcription. During stationary phase, when the fungus is no longer actively dividing and has exhausted exogenous nutrients, the fungus can metabolize energy stores, such as starch, glycogen, lipids, and peptides, for cell turnover and maintenance of cell integrity, causing high enrichment of energy and metabolic functional categories (Fig. 6) (32). Cellular components can be broken down and transported from older internal compartments to the newer peripheral hyphae, allowing limited growth, which may account for the enrichment of protein fate, transport, transcription, and protein binding at 48 h of growth. This ultimately leads to autolysis and cell death (32). The lack of the protein biosynthesis category during stationary phase is consistent with the irreversible loss or slowing of *Aspergillus niger* protein synthesis during fungal aging and autolysis (32).

Only the acetyl-CoA carboxylase, associated with fatty acid biosynthesis, had higher reactivity in the presence of HS at 24 h. Acetyl-CoA carboxylase catalyzes the committed step in fatty acid biosynthesis, and the *Saccharomyces cerevisiae* (*ACC1*) and *Aspergillus nidulans* (*accA*) orthologs are necessary for growth (53, 54) and have a role in transport of proteins into the nucleus (55). Its high reactivity in AMM + HS 24 h is consistent with log phase growth, where carbohydrates and energy are plentiful and the fungus requires fatty acids for phospholipid biosynthesis (53). The smaller -fold difference between 48 and 24 h in HS culture may correspond with nutrient depletion and no additional accumulation of biomass during stationary phase. Notably, the acetyl-CoA carboxylase activity increases over time in minimal medium culture such that there is no significant change in enzyme reactivity between the presence and absence of HS at 48 h (Table 2). The large fc (~14) observed in the AMM 24 h and AMM 48 h reflects higher reactivity at mid-log phase growth than at late lag phase/early log phase growth (54). The early high reactivity of the *A. fumigatus* acetyl-CoA carboxylase in the presence of HS components may provide an opportunity for early detection of fungal load in host tissue (56).

At stationary phase (48 h) in HS culture, two unique proteins were observed (supplemental Table S2*C*). The *ark1* is an aldehyde reductase that converts acetaldehyde to ethanol in the gluconeogenesis/glycolysis and pyruvate metabolism cycles (31). The unique observation and high reactivity of this protein in the AMM + HS at 48 h suggests up-regulation of fermentation possibly due to O_2 limitation in aging liquid culture medium (57). Furthermore, the *akr1* transcript was up-regulated in the presence of reactive oxygen species (ROS) and neutrophils (58, 59), suggesting a role in response to oxidative stress. The *glr1* is a glutathione oxidoreductase whose ortholog helps balance glutathione and glutathione disulfide ratios and redox homeostasis in *S. cerevisiae* during stationary phase (60). In the phytopathogenic fungus *Fusarium decemcellulare*, *glr* activity increased by 5-fold during stationary phase (61). The high enzyme reactivity of these two unique proteins may be associated with a link between metabolism/respiration and ROS generation (62). A connection between up-regulation of glycolysis, ethanol production, and ROS formation due to increased aerobic respiration in an *A. fumigatus* GTPase RacA mutant has been made previously (63). The observation of these unique enzymes using ABPP may be useful for diagnostic purposes because it is known that conidia and hypha encounter

ROS (64), oxygen limitation (65), and alternative carbon sources during infection (66).

As the fungus aged in minimal medium, the functional pathways with high activity were quite different from those during early growth. At 24 h of growth, the log phase is just beginning, and the high level of metabolism, energy production, biosynthesis, and transcription-associated protein activity correlates with initial exit from dormancy (51), germ tube elongation, and hyphal extension (32). During continued log phase, the cell cycle regulators *H3* and *SkpA* had high reactivity because during log phase growth hyphae septation and mitosis are occurring rapidly (32). The *S. cerevisiae* ortholog of *H3* is crucial for activating the spindle assembly checkpoint in response to errors during mitosis (67). Likewise, the *S. cerevisiae* ortholog *Skp1p* is necessary for cell cycle progression and may play a regulatory role in activation of a cell cycle checkpoint (68). Finally, as the medium nutrients are depleted and the fungus can no longer maintain exponential growth, the fungus approaches stationary phase, and enzymes associated with stress response and secondary metabolism are highly enriched (Table 2). The *nrps14*, Glim-Like *O*-methyltransferase (AFUA_3G11920), *Erg1*, oxidoreductase 2OG-Fe (II) oxygenase family (AFUA_3G00800), HAD superfamily hydrolase (AFUA_5G08270, down regulated under hypoxia), Ure2-like glutathione Stransferase (AFUA_4G14530), and a conserved hypothetical protein (AFUA_8G00430) transcripts were altered in response to hypoxia. The fructosyl amino acid oxidase (AFUA_6G03440) transcript was up regulated in the presence of the antifungal drug voriconazole. It is intriguing that approaching stationary phase induces an enzyme reactivity response similar to hypoxia and azole responses.

A link between aging fungal culture and oxidative stress has been observed previously (69). In *S. cerevisiae*, tight control of cellular redox homeostasis, including mitochondrial production of ROS, is necessary for survival as the organism approaches and enters stationary growth phase (60). Six proteins with high reactivity at 48 h in minimal medium, the *fgaCat*, *Arp2*, cytochrome P450 (AFUA_5G02610), OrdA-like cytochrome P450 oxidoreductase (AFUA_8G00510), and flavin-binding monooxygenase-like protein (AFUA_4G09220), are annotated with redox regulatory processes, response to oxidative stress, and hydrogen peroxide catabolic processes and may play a role in controlling cellular redox homeostasis in *A. fumigatus* (Table 2). The high reactivity of the oxidative stress response regulator *MpkA* under these conditions supports this hypothesis (70). ROS accumulation may trigger an apoptotic response in *A. fumigatus* as it enters stationary phase, and studies found that a rapid loss of mycelia viability (>95%) occurred soon after stationary phase began (71). As stationary phase begins, the high levels of enzyme reactivity associated with oxidative stress correlates could be due to increasing ROS accumulation.

A. fumigatus can undergo autophagy in response to aging and nutrient depletion stress (72). This process allows limited growth of the fungus at the mycelium periphery to enable foraging of new nutritional sources in the environment and conidiation in response to starvation (73). Conidia are more robust to environmental stressors and can be a means of survival after nutrients cannot sustain growth (74). The two conidial melanin pigment biosynthetic proteins *Arp1* and *Ayg2* were previously found to be up-regulated in conidia when compared with mycelia and in swollen conidia at 4 h of germination (51, 75). In addition to possible roles in oxidative stress response, the high reactivity of these proteins at 48 h in minimal growth suggests that *A. fumigatus* is producing conidia under these conditions. In contrast, these pigment proteins were not significantly changing over time in HS culture, and at each time point enzyme reactivity levels were higher in minimal medium. This suggests that HS culture conidia formation is suppressed.

The drastic differences in protein reactivity during the aging process in the presence and absence of HS were visualized by mapping confidently identified proteins onto KEGG pathways. The generality of probe **1** allowed capture of many proteins within primary metabolism and energy pathways (Fig. 6). By using heat maps to express fc, we observed that proteins involved in the glycolysis/gluconeogenesis, glyoxylate and TCA pathways have greater probe reactivity over time in HS culture than in minimal medium. The high reactivity of pyruvate decarboxylase *pdc* and alcohol dehydrogenase *adh1* within these pathways is consistent with a switch from aerobic respiration to fermentation (65). High reactivity of enzymes within the gluconeogenesis pathway and TCA pathway is further evidence that ethanol is being used as a carbon source (75, 76). The apparent switch to fermentation processes at 48 h of growth may be due to reduced dissolved O_2 levels in the medium (57) and reduced efficient transfer of O_2 through the pellet (32), thereby creating a hypoxic-like environment. Due to the differences in growth state between the culture conditions at 48 h, it is difficult to determine which effects are attributable to the availability of human serum components and which result from stationary phase growth. Instead, the enhanced biomass production, early log phase, and stationary phase are a direct result of HS culture. A comparison of biomass obtained from stationary phase in AMM and AMM + HS culture would show if these proteins and the metabolic change during stationary phase are truly unique to HS culture or growth phase-dependent.

It is apparent that ABPP using **1** and **2** coupled with a label-free quantitative AMT tag proteomics approach showed different active functional states between two growth conditions and two time points and is a powerful tool in analyzing a complex filamentous fungus. As expected, HS induces early log phase growth and an increase in biomass production. Whereas metabolism and energy function are greatly increasing from mid-log phase growth to stationary phase in the presence of HS, in the absence of HS, the fungus appears to be responding to stress as it approaches stationary phase. The low reactivity of stress response and secondary metabolism proteins observed in HS culture when compared with AMM suggests that *A. fumigatus* is not encountering the same stressors during growth in HS, possibly due to the ability to use nutrients present in HS. The ability of *A. fumigatus* to adapt well to a host environment is considered one of its virulence factors, and our study clearly shows adaptation to a complex environment. Fur-

thermore, the high reactivity of stress response proteins observed from minimal medium biomass at 48 h provides some insight into functional activity during nutrient deprivation and the aging process. Because exogenous stressors were not applied in our experiment, it would be beneficial to observe enzyme reactivity in the presence of antifungal agents and under hypoxic conditions.

Our results show on a protein reactivity level biological and metabolic pathways and mechanisms of *A. fumigatus* likely to be operative in opportunistic infections because in the human lung, the fungus encounters stress due to immune response and alternative carbon sources such as human proteins and lipids. Furthermore, the identification of highly reactive unique enzymes, indicating fungal presence, load, and fungal homeostasis, may provide an opportunity for diagnosis of IA. In combination with these methods, cross-species comparisons and incorporation of host responses to *Aspergillus* infection could yield further insights into the complexity of *A. fumigatus* pathogenesis during IA.

Acknowledgments—We thank the Biological Separations and Mass Spectrometry group and the Chemical and Biological Processes Development Group for helpful discussions and critical reading of the manuscript.

REFERENCES

1. Latgé, J. P. (1999) *Aspergillus fumigatus* and aspergillosis. *Clin. Microbiol. Rev.* **12,** 310–350
2. Dagenais, T. R., and Keller, N. P. (2009) Pathogenesis of *Aspergillus fumigatus* in invasive aspergillosis. *Clin. Microbiol. Rev.* **22,** 447–465
3. Michael, A., Pfaller, P. G., Wingard, J. R. (2006) Invasive fungal pathogens. Current epidemiological trends. *Clin. Infect. Dis.* **43,** S3–S14
4. Lai, C. C., Tan, C. K., Huang, Y. T., Shao, P. L., and Hsueh, P. R. (2008) Current challenges in the management of invasive fungal infections. *J. Infect. Chemother.* **14,** 77–85
5. Hummel, M., and Buchheidt, D. (2007) Molecular and serological diagnosis of invasive aspergillosis. New answers to old questions? *Mycoses* **50,** 18–23
6. Denning, D. W., and Hope, W. W. (2010) Therapy for fungal diseases. Opportunities and priorities. *Trends Microbiol.* **18,** 195–204
7. Rhodes, J. C., and Askew, D. S. (2010) *Aspergillus fumigatus.* in *Cellular and Molecular Biology of Filamentous Fungus* (Borkovich, K. A., and Ebbole, D. J., eds) pp. 697–716, American Society for Microbiology, Washington D. C.
8. Hohl, T.M., and Feldmesser, M. (2007) *Aspergillus fumigatus*. Principles of pathogenesis and host defense. *Eukaryot. Cell* **6,** 1953–1963
9. Bhabhra, R., and Askew, D.S. (2005) Thermotolerance and virulence of *Aspergillus fumigatus*. Role of the fungal nucleolus. *Med. Mycol.* **43,** S87–S93
10. Willger, S. D., Grahl, N., and Cramer, R. A. (2009) *Aspergillus fumigatus* metabolism. Clues to mechanisms of *in vivo* fungal growth and virulence. *Med. Mycol.* **47,** S72–S79
11. Oliver, B. G., Panepinto, J. C., Askew, D. S., and Rhodes, J. C. (2002) cAMP alteration of growth rate of *Aspergillus fumigatus* and *Aspergillus niger* is carbon source-dependent. *Microbiology* **148,** 2627–2633
12. Fleck, C. B., Schöbel, F., and Brock, M. (2011) Nutrient acquisition by pathogenic fungi. Nutrient availability, pathway regulation, and differences in substrate utilization. *Int. J. Med. Microbiol.* **301,** 400–407
13. Schoberle, T., and May, G. (2007) Fungal genomics. A tool to explore central metabolism of *Aspergillus fumigatus* and its role in virulence. *Adv. Genet.* **57,** 263–283
14. Kniemeyer, O. (2011) Proteomics of eukaryotic microorganisms. The medically and biotechnologically important fungal genus *Aspergillus*. *Proteomics* **11,** 3232–3243
15. Lenz, T., Fischer, J. J., and Dreger, M. (2011) Probing small molecule-protein interactions. A new perspective for functional proteomics. *J. Proteomics* **75,** 100–115
16. Cravatt, B. F., Wright, A. T., and Kozarich, J. W. (2008) Activity-based protein profiling. From enzyme chemistry to proteomic chemistry. *Annu. Rev. Biochem.* **77,** 383–414
17. Zimmer, J. S., Monroe, M. E., Qian, W. J., and Smith, R. D. (2006) Advances in proteomics data analysis and display using an accurate mass and time tag approach. *Mass Spectrom. Rev.* **25,** 450–482
18. Gifford, A. H., Klippenstein, J. R., and Moore, M. M. (2002) Serum stimulates growth of and proteinase secretion by *Aspergillus fumigatus*. *Infect. Immun.* **70,** 19–26
19. Hissen, A. H., Chow, J. M., Pinto, L. J., and Moore, M. M. (2004) Survival of *Aspergillus fumigatus* in serum involves removal of iron from transferrin. The role of siderophores. *Infect. Immun.* **72,** 1402–1408
20. Toyotome, T., Yamaguchi, M., Iwasaki, A., Watanabe, A., Taguchi, H., Qin, L., Watanabe, H., and Kamei, K. (2012) Fetuin A, a serum component, promotes growth and biofilm formation by *Aspergillus fumigatus*. *Int. J. Med. Microbiol.* **302,** 108–116
21. Rodrigues, A. G., Araujo, R., and Pina-Vaz, C. (2005) Human albumin promotes germination, hyphal growth, and antifungal resistance by *Aspergillus fumigatus*. *Med. Mycol.* **43,** 711–717
22. Shimizu, K., and Keller, N.P. (2001) Genetic involvement of a cAMP-dependent protein kinase in a G protein signaling pathway regulating morphological and chemical transitions in *Aspergillus nidulans*. *Genetics* **157,** 591–600
23. Kägi, J. H., and Vallee, B. L. (1960) The role of zinc in alcohol dehydrogenase. *J. Biol. Chem.* **235,** 3188–3192
24. Livesay, E. A., Tang, K., Taylor, B. K., Buschbach, M. A., Hopkins, D. F., LaMarche, B. L., Zhao, R., Shen, Y., Orton, D. J., Moore, R. J., Kelly, R. T., Udseth, H. R., and Smith, R. D. (2008) Fully automated four-column capillary LC-MS system for maximizing throughput in proteomic analyses. *Anal. Chem.* **80,** 294–302
25. Yates, J. R., 3rd, Eng, J. K., McCormack, A. L., and Schieltz, D. (1995) Method to correlate tandem mass spectra of modified peptides to amino acid sequences in the protein database. *Anal. Chem.* **67,** 1426–1436
26. Kim, S., Gupta, N., and Pevzner, P. A. (2008) Spectral probabilities and generating functions of tandem mass spectra. A strike against decoy databases. *J. Proteome Res.* **7,** 3354–3363
27. Monroe, M. E., Tolić, N., Jaitly, N., Shaw, J. L., Adkins, J. N., and Smith, R. D. (2007) VIPER. An advanced software package to support high-throughput LC-MS peptide identification. *Bioinformatics* **23,** 2021–2023
28. Polpitiya, A. D., Qian, W. J., Jaitly, N., Petyuk, V. A., Adkins, J. N., Camp, D. G., 2nd, Anderson, G. A., and Smith, R. D. (2008) DAnTE. A statistical tool for quantitative analysis of -omics data. *Bioinformatics* **24,** 1556–1558
29. Arnaud, M. B., Chibucos, M. C., Costanzo, M. C., Crabtree, J., Inglis, D. O., Lotia, A., Orvis, J., Shah, P., Skrzypek, M. S., Binkley, G., Miyasato, S. R., Wortman, J. R., and Sherlock, G. (2010) The Aspergillus Genome Database, a curated comparative genomics resource for gene, protein, and sequence information for the Aspergillus research community. *Nucleic Acids Res.* **38,** D420–D427
30. Priebe, S., Linde, J., Albrecht, D., Guthke, R., and Brakhage, A. A. (2011) FungiFun. A web-based application for functional categorization of fungal genes and proteins. *Fungal Genet. Biol.* **48,** 353–358
31. Kanehisa, M., Goto, S., Sato, Y., Furumichi, M., and Tanabe, M. (2012) KEGG for integration and interpretation of large scale molecular data sets. *Nucleic Acids Res.* **40,** D109–D114
32. Papagianni, M. (2004) Fungal morphology and metabolite production in submerged mycelial processes. *Biotechnol. Adv.* **22,** 189–259
33. Liu, S., Zhou, B., Yang, H., He, Y., Jiang, Z. X., Kumar, S., Wu, L., and Zhang, Z. Y. (2008) Aryl vinyl sulfonates and sulfones as active site-directed and mechanism-based probes for protein-tyrosine phosphatases. *J. Am. Chem. Soc.* **130,** 8251–8260
34. Weerapana, E., Simon, G. M., and Cravatt, B. F. (2008) Disparate proteome reactivity profiles of carbon electrophiles. *Nat. Chem. Biol.* **4,**

405–407
35. Barglow, K. T., and Cravatt, B. F. (2004) Discovering disease-associated enzymes by proteome reactivity profiling. *Chem. Biol.* **11,** 1523–1531
36. Böttcher, T., and Sieber, S.A. (2008) β-Lactones as privileged structures for the active-site labeling of versatile bacterial enzyme classes. *Angew. Chem. Int. Ed. Engl.* **47,** 4600–4603
37. Gillet, L. C., Namoto, K., Ruchti, A., Hoving, S., Boesch, D., Inverardi, B., Mueller, D., Coulot, M., Schindler, P., Schweigler, P., Bernardi, A., and Gil-Parrado, S. (2008) In-cell selectivity profiling of serine protease inhibitors by activity-based proteomics. *Mol. Cell Proteomics* **7,** 1241–1253
38. Schmidinger, H., Hermetter, A., and Birner-Gruenberger, R. (2006) Activity-based proteomics. Enzymatic activity profiling in complex proteomes. *Amino Acids* **30,** 333–350
39. Köster, H., Little, D. P., Luan, P., Muller, R., Siddiqi, S. M., Marappan, S., and Yip, P. (2007) Capture compound mass spectrometry. A technology for the investigation of small molecule protein interactions. *Assay Drug Dev. Technol.* **5,** 381–390
40. Wallwey, C., Matuschek, M., Xie, X. L., and Li, S. M. (2010) Ergot alkaloid biosynthesis in *Aspergillus fumigatus*. Conversion of chanoclavine-I aldehyde to festuclavine by the festuclavine synthase FgaFS in the presence of the old yellow enzyme FgaOx3. *Org. Biomol. Chem.* **8,** 3500–3508
41. Tsai, H. F., Wheeler, M. H., Chang, Y. C., and Kwon-Chung, K. J. (1999) A developmentally regulated gene cluster involved in conidial pigment biosynthesis in *Aspergillus fumigatus*. *J. Bacteriol.* **181,** 6469–6477
42. Maiya, S., Grundmann, A., Li, X., Li, S. M., and Turner, G. (2007) Identification of a hybrid PKS/NRPS required for pseurotin A biosynthesis in the human pathogen *Aspergillus fumigatus*. *ChemBioChem* **8,** 1736–1743
43. Lodeiro, S., Xiong, Q., Wilson, W. K., Ivanova, Y., Smith, M. L., May, G. S., and Matsuda, S. P. (2009) Protostadienol biosynthesis and metabolism in the pathogenic fungus *Aspergillus fumigatus*. *Org. Lett.* **11,** 1241–1244
44. da Silva Ferreira, M. E., Malavazi, I., Savoldi, M., Brakhage, A. A., Goldman, M. H., Kim, H. S., Nierman, W. C., and Goldman, G. H. (2006) Transcriptome analysis of *Aspergillus fumigatus* exposed to voriconazole. *Curr. Genet.* **50,** 32–44
45. Vödisch, M., Scherlach, K., Winkler, R., Hertweck, C., Braun, H. P., Roth, M., Haas, H., Werner, E. R., Brakhage, A. A., and Kniemeyer, O. (2011) Analysis of the *Aspergillus fumigatus* proteome reveals metabolic changes and the activation of the pseurotin A biosynthesis gene cluster in response to hypoxia. *J. Proteome Res.* **10,** 2508–2524
46. Tsai, H. F., Chang, Y. C., Washburn, R. G., Wheeler, M. H., and Kwon-Chung, K. J. (1998) The developmentally regulated *alb1* gene of *Aspergillus fumigatus*. Its role in modulation of conidial morphology and virulence. *J. Bacteriol.* **180,** 3031–3038
47. Valiante, V., Heinekamp, T., Jain, R., Härtl, A., and Brakhage, A.A. (2008) The mitogen-activated protein kinase MpkA of *Aspergillus fumigatus* regulates cell wall signaling and oxidative stress response. *Fungal Genet. Biol.* **45,** 618–627
48. Ferreira, M. E., Colombo, A. L., Paulsen, I., Ren, Q., Wortman, J., Huang, J., Goldman, M. H., and Goldman, G. H. (2005) The ergosterol biosynthesis pathway, transporter genes, and azole resistance in *Aspergillus fumigatus*. *Med. Mycol.* **43,** S313–S319
49. Roush, W. R., Gwaltney, S. L., Cheng, J., Scheidt, K. A., McKerrow, J. H., and Hansell, E. (1998) Vinyl sulfonate esters and vinyl sulfonamides. Potent, irreversible inhibitors of cysteine proteases. *J. Am. Chem. Soc.* **120,** 10994–10995
50. Krappmann, S. (2003) in *Aspergillus fumigatus* and Aspergillosis (Latgé, J.-P., and Steinbach, W. J., eds) pp. 63–74, ASM Press, Washington DC
51. Cagas, S. E., Jain, M. R., Li, H., and Perlin, D. S. (2011) The proteomic signature of *Aspergillus fumigatus* during early development. *Mol. Cell Proteomics* **10,** M111.010108
52. McDonagh, A., Fedorova, N.D., Crabtree, J., Yu, Y., Kim, S., Chen, D., Loss, O., Cairns, T., Goldman, G., Armstrong-James, D., Haynes, K., Haas, H., Schrettl, M., May, G., Nierman, W. C., and Bignell, E. (2008) Sub-telomere-directed gene expression during initiation of invasive aspergillosis. *PLoS Pathog.* **4,** e1000154
53. Hasslacher, M., Ivessa, A. S., Paltauf, F., and Kohlwein, S. D. (1993) Acetyl-CoA carboxylase from yeast is an essential enzyme and is regulated by factors that control phospholipid metabolism. *J. Biol. Chem.* **268,** 10946–10952
54. Morrice, J., MacKenzie, D. A., Parr, A. J., and Archer, D. B. (1998) Isolation and characterization of the acetyl-CoA carboxylase gene from *Aspergillus nidulans*. *Curr. Genet.* **34,** 379–385
55. Gao, H., Sumanaweera, N., Bailer, S. M., and Stochaj, U. (2003) Nuclear accumulation of the small GTPase Gsp1p depends on nucleoporins Nup133p, Rat2p/Nup120p, Nup85p, Nic96p, and the acetyl-CoA carboxylase Acc1p. *J. Biol. Chem.* **278,** 25331–25340
56. Dorr, P. K., Parkinson, T., and Bulawa, C. E. (2003) U.S. Patent 6, 514, 726B
57. Taubitz, A., Bauer, B., Heesemann, J., and Ebel, F. (2007) Role of respiration in the germination process of the pathogenic mold *Aspergillus fumigatus*. *Curr. Microbiol.* **54,** 354–360
58. Sugui, J. A., Kim, H. S., Zarember, K. A., Chang, Y. C., Gallin, J. I., Nierman, W. C., and Kwon-Chung, K. J. (2008) Genes differentially expressed in conidia and hyphae of *Aspergillus fumigatus* upon exposure to human neutrophils. *PLoS ONE* **3,** e2655
59. Oosthuizen, J. L., Gomez, P., Ruan, J., Hackett, T. L., Moore, M. M., Knight, D. A., and Tebbutt, S. J. (2011) Dual organism transcriptomics of airway epithelial cells interacting with conidia of *Aspergillus fumigatus*. *PLoS ONE* **6,** e20527
60. Drakulic, T., Temple, M. D., Guido, R., Jarolim, S., Breitenbach, M., Attfield, P. V., and Dawes, I. W. (2005) Involvement of oxidative stress response genes in redox homeostasis, the level of reactive oxygen species, and aging in *Saccharomyces cerevisiae*. *FEMS Yeast Res.* **5,** 1215–1228
61. Gessler, N., Aver'yanov, A., and Belozerskaya, T. A. (2007) Reactive oxygen species in regulation of fungal development. *Biochemistry* **72,** 1091–1109
62. Bai, Z., Harvey, L. M., and McNeil, B. (2003) Oxidative stress in submerged cultures of fungi. *Crit. Rev. Biotechnol.* **23,** 267–302
63. Li, H., Barker, B. M., Grahl, N., Puttikamonkul, S., Bell, J. D., Craven, K. D., and Cramer, R. A. (2011) The small GTPase RacA mediates intracellular reactive oxygen species production, polarized growth, and virulence in the human fungal pathogen *Aspergillus fumigatus*. *Eukaryot. Cell* **10,** 174–186
64. McCormick, A., Loeffler, J., and Ebel, F. (2010) *Aspergillus fumigatus*. Contours of an opportunistic human pathogen. *Cell. Microbiol.* **12,** 1535–1543
65. Grahl, N., Puttikamonkul, S., Macdonald, J. M., Gamcsik, M. P., Ngo, L. Y., Hohl, T. M., and Cramer, R. A. (2011) *In vivo* hypoxia and a fungal alcohol dehydrogenase influence the pathogenesis of invasive pulmonary aspergillosis. *PLoS Pathog.* **7,** e1002145
66. Ibrahim-Granet, O., Dubourdeau, M., Latgé, J. P., Ave, P., Huerre, M., Brakhage, A. A., and Brock, M. (2008) Methylcitrate synthase from *Aspergillus fumigatus* is essential for manifestation of invasive aspergillosis. *Cell. Microbiol.* **10,** 134–148
67. Luo, J., Xu, X., Hall, H., Hyland, E. M., Boeke, J. D., Hazbun, T., and Kuo, M. H. (2010) Histone H3 exerts a key function in mitotic checkpoint control. *Mol. Cell. Biol.* **30,** 537–549
68. Connelly, C., and Hieter, P. (1996) Budding yeast SKP1 encodes an evolutionarily conserved kinetochore protein required for cell cycle progression. *Cell* **86,** 275–285
69. SáMi, L., Emri, T., and Pócsi, I. (2001) Autolysis and aging of *Penicillium chrysogenum* cultures under carbon starvation. Glutathione metabolism and formation of reactive oxygen species. *Mycol. Res.* **105,** 1246–1250
70. Jain, R., Valiante, V., Remme, N., Docimo, T., Heinekamp, T., Hertweck, C., Gershenzon, J., Haas, H., and Brakhage, A. A. (2011) The MAP kinase MpkA controls cell wall integrity, oxidative stress response, gliotoxin production, and iron adaptation in *Aspergillus fumigatus*. *Mol. Microbiol.* **82,** 39–53
71. Mousavi, S. A., and Robson, G. D. (2003) Entry into the stationary phase is associated with a rapid loss of viability and an apoptotic-like phenotype in the opportunistic pathogen *Aspergillus fumigatus*. *Fungal Genet. Biol.* **39,** 221–229
72. Palmer, G. E., Askew, D. S., and Williamson, P. R. (2008) The diverse roles of autophagy in medically important fungi. *Autophagy* **4,** 982–988

73. Richie, D. L., Fuller, K. K., Fortwendel, J., Miley, M. D., McCarthy, J. W., Feldmesser, M., Rhodes, J. C., and Askew, D. S. (2007) Unexpected link between metal ion deficiency and autophagy in *Aspergillus fumigatus*. *Eukaryot. Cell* **6,** 2437–2447
74. Adams, T. H., Wieser, J. K., and Yu, J. H. (1998) Asexual Sporulation in *Aspergillus nidulans*. *Microbiol. Mol. Biol. Rev.* **62,** 35–54
75. Teutschbein, J., Albrecht, D., Pötsch, M., Guthke, R., Aimanianda, V., Clavaud, C., Latgé, J. P., Brakhage, A. A., and Kniemeyer, O. (2010) Proteome profiling and functional classification of intracellular proteins from conidia of the human-pathogenic mold *Aspergillus fumigatus*. *J. Proteome Res.* **9,** 3427–3442
76. Kniemeyer, O., Lessing, F., Scheibner, O., Hertweck, C., and Brakhage, A. (2006) Optimization of a two-dimensional gel electrophoresis protocol for the human-pathogenic fungus *Aspergillus fumigatus*. *Curr. Genet.* **49,** 178–189